




Automatic Detection of Drowsiness in EEG Records Based on Machine Learning Approaches

Afef Abidi^{1,2,3} · Khaled Ben Khalifa^{1,4}  · Ridha Ben Cheikh^{1,5} · Carlos Alberto Valderrama Sakuyama³ · Mohamed Hedi Bedoui¹

Accepted: 20 April 2022

© The Author(s), under exclusive licence to Springer Science+Business Media, LLC, part of Springer Nature 2022

Abstract

Drowsy driving is a major cause of road accidents. Traffic accidents can be prevented by discriminating between driver states of alertness and drowsiness. This paper presents an efficient system for drowsiness detection based on EEG signals. The proposed system is efficient in providing consistent results regardless of the inherent characteristics of drivers. Our method is based on features extracted from well-defined sub-bands. These sub-bands obtained using a tunable Q-factor wavelet transform. The use of sub-bands solves the problem of interpersonal variability of EEG recordings, which is a major problem in detecting drowsiness. In addition, the use of kernel principal component analysis reduces the size of the features extracted from EEG signals without degrading the accuracy. Indeed, a single differential EEG channel with a minimal number of carefully selected features is sufficient to provide a fast, convenient, and accurate detection system. For drowsiness recognition, two different machine learning techniques, K-nearest neighbours and support vector machines, are proposed. The latter consists of a learning module for medical diagnosis based on EEG signals from a set of laboratory subjects. Laboratory conditions help identify characteristic and common features. These preparatory parameters make it possible to provide a real-time adaptive drowsiness diagnosis by assessing the driver's condition every second. By customizing the system, it can detect drowsiness with an accuracy of approximately 94%.

Keywords Drowsiness detection · EEG · KPCA · TQWT · SVM

✉ Khaled Ben Khalifa
khaled.benkhalifa@issatso.rnu.tn

¹ Technology and Medical Imaging Laboratory, Faculty of Medicine Monastir, University of Monastir, 5019 Monastir, Tunisia

² National Engineering School of Sousse, University of Sousse, BP 264 Erriyadh, 4023 Sousse, Tunisia

³ Department of Electronics and Microelectronics (SEMi), University of Mons, 7000 Mons, Belgium

⁴ Institut Supérieur des Sciences Appliquées et de Technologie de Sousse, Université de Sousse, 4003 Sousse, Tunisia

⁵ Service d'explorations fonctionnelles du système nerveux, CHU Sahloul, 4054 Sousse, Tunisia

1 Introduction

The term vigilance is defined differently according to scientific disciplines (neurophysiology, psychology, or ergonomics). Etymologically, this means awakening. We attribute the designation of vigilance states to the different levels of the wake-sleep cycle. It can be related to the level of cerebral activity, and thus, it underpins all mental operations, from the simple detection of information to the development and expression of behavior. However, the level of performance increases with alertness to an optimum level beyond which performance drops. This makes it possible to understand that high (stress) or low vigilance (e.g., caused by a lack of sleep) can affect performance [1].

The spontaneous electrical activity of the cortex is dynamic, stochastic, nonlinear, and nonstationary. The sleep-wake transition, which differs from subject to subject, is marked by sudden variations in the frequency and amplitude of the EEG signal. According to [2], the transition from wakefulness to sleep is manifested by the appearance of an intermediate stage called somnolence.

Drowsiness has been recognized in recent years as a very important and significant factor in increasing the number of road accidents. According to the latest published statistics, drowsy driving accounts for 20% of road accidents worldwide [3]. A survey on the indicators of hypo-vigilance, particularly fatigue, quantified by the appearance of the drowsiness stage, has allowed us to present an overview of the various approaches used for the detection of this state. In this regard, we can classify the most popular detection approaches into three main categories: vehicle movements, driver behaviors, and physiological sensing.

The first category is based on the movements of the vehicle [4], such as the detection of lane changes or the pressure of the driving pedal [5, 6]. These measures show a high potential for detecting drowsiness. Nevertheless, their reliability is affected by vehicle type, driving expertise, and environmental and road conditions [7]. For assisted driving, it is more complicated to assess these factors because the vehicle is being monitored by an automated system.

The second category focuses on the behavior of the driver himself, essentially analyzing his yawning, closing, and blinking of eyes (PERCLOS: "PERcentage of eyelid CLOSure"), or the head pose, among other similar movements [4]. This process is quite effective but not easy to market, as drivers do not appreciate being constantly supervised by a camera [8]. Nevertheless, there are many commercial products ranging from camera-based methods [9, 10] to devices worn over glasses [11]. However, different flashing frequencies and amplitudes can affect the monitoring quality [12]. In addition, insufficient lighting and sunglasses can limit the performance of monitoring systems [4].

The last category of assessing drowsiness includes systems relying on the exploitation of physiological characteristics, including EEG [13–15], Electrocardiogram (ECG) [16], and Electrooculogram (EOG) [17]. These are generally identified as objective data-driven quantification systems. The objective assessment of drowsiness is carried out by specialized laboratories capable of performing analyses such as the iterative awakening preservation test with data collected in real or deferred time [10, 18]. According to [19], owing to its excellent time resolution and sensitivity to fatigue detection, EEG provides better results than other physiological signals. Although effective, this technique is cumbersome, as several electrodes are usually required to improve accuracy and robustness. EEG signals are formed by several rhythms representing various mental states, such as drowsiness and vigilance. Bearing this in mind, a variety of studies have attempted to perform EEG-based parameter extraction using

66 different signal processing techniques in order to choose the most relevant parameters to
67 accurately detect drowsiness.

68 Focusing on objective data-driven quantification systems, the most interesting methods
69 proposed in several papers involve the analysis of EEG signals based on Fast Fourier Trans-
70 form (FFT), filtering techniques, wavelet transform, direct feature extraction, and empirical
71 mode decomposition. FFT-based methods suffer from localization issues [20]. Filtering
72 requires the selection of precise filtering limits. Wavelet-based techniques imply the selection
73 of an appropriate mother wavelet and decomposition levels [8]. Decomposition in the empir-
74 ical mode is entirely based on experiments and requires mathematical modelling. Therefore,
75 there is a great need to carefully decompose and retrieve information [21]. Nevertheless, the
76 Tunable Q-factor Wavelet Transform (TQWT) does not require the selection of the wavelet
77 function [22]. Hence, the particular interest in TQWT, very useful for obtaining an efficient
78 and sparse representation of signals.

79 Several studies have reported on the automated evaluation of vigilance fluctuations based
80 on the analysis of EEG signals. In this context, a signal classifier plays a very important role in
81 terms of accuracy and reliability. Several classifiers have been proposed for related or similar
82 scenarios. In [23], a Multi-Layer Perceptron (MLP) and a Learning Vector Quantization
83 (LVQ) network was trained to classify six vigilance states from 30-s EEG epochs in infants.
84 In this study, recordings of three infants were used for training and one for testing. The
85 classification results are almost equivalent for both networks. The authors in [24] suggested
86 a spectral analysis approach while adopting a multilayer neural network for classification.
87 The aim was to explore the correlation between the spectral EEG signal and the level of
88 alertness, quantified by an auditory test. In [25], a radial basis function (RBF) was used to
89 classify the alertness levels of 12 subjects by exploiting fragments of their EEG signals.
90 The authors used the coefficients of an autoregressive model as input parameters. In [5], the
91 authors mapped wake-sleep transitions over 1.28 s EEG epochs while taking into account
92 artifacts using Kohonen's self-organizing maps.

93 Perhaps considered the latest complete studies, the authors in [26] exploited three super-
94 vised learning connectionist models: a multilayer feed-forward network, a linear neural
95 network, and an LVQ. Note that the three approaches were used to identify the two states
96 awake and drowsy using 14 EEG signal derivations from 12 subjects. It should also be
97 noted that none of the adopted approaches considered the appearance of artifacts in the EEG
98 signals that were expertly removed. In [27], the authors put forward a drowsiness recogni-
99 tion application using attention and meditation signals from NeuroSky features; the signals
100 were classified using the (KNN). The best results of all tests yielded an accuracy rate of
101 95.24%. In [28], the authors adopted the KNN to detect driving fatigue and alert states using
102 EEG derivation. The results in terms of sensitivity and specificity were 68.31% and 90.43%,
103 respectively.

104 In recent years, Deep Learning (DL) approaches have demonstrated abilities in terms
105 of object identification and EEG prediction. Thus, Almogbel et al. [29] used four EEG
106 derivations collected from a single subject and a Convolutional Neural Network (CNN) to
107 estimate the workload based on EEG, achieving the highest accuracy of 95.3%. In [13], the
108 authors proposed a new approach to predict the alertness states of individuals by analyzing
109 EEG signals using DL architectures. In this study, two types of networks, 1D-UNet and 1D-
110 UNet-Long Short-Term Memory (1D-UNet-LSTM), were employed. The per-class average
111 precision and recall were 86% for 1D-UNet and 85% for 1D-UNet-LSTM.

112 Many researchers have utilized Support Vector Machines (SVMs) to classify and detect
113 drowsiness phases from EEG signals. In [18], the authors extracted four frequency features
114 from the EEG signal and then used an SVM classifier for fatigue detection, which gave an

115 excellent classification rate. In [30], the authors used nine features extracted from 11 EEG
116 channels and an SVM-based classifier to distinguish drowsiness from wakefulness. The accu-
117 racy achieved by this system was approximately 95%. In [31], the authors opted for an SVM
118 classifier to distinguish between vigilance states. The authors' results highlighted the consid-
119 erable ability of portable EEG devices to discriminate among various cognitive states under
120 various conditions. Karuppusamy and Kang [32] used 14 EEG derivations collected from
121 OpenBCI headsets. The authors manually labelled the EEG sequences based on the eyeblink
122 images. The maximum performance achieved using this approach is approximately 81%.
123 The authors of [33] used a wearable headband (MUSE) for real-time drowsiness detection
124 in drivers. Based on the EEG spectral characteristics, the authors achieved a performance of
125 74% in cross-validating subjects with SVM. The authors also detected drowsiness using blink
126 duration parameters. The efficiency of the blink parameters was found to be less than that
127 of the spectral analysis. In [34], the authors put forward a system for detecting drowsiness
128 based on EEG signals using a linear SVM for classification. This solution made it possi-
129 ble to obtain an average precision of 99.1%. The proposed system was very complex and
130 contained several blocks, which made it very hard to be applied in real time. In addition,
131 the authors extracted 32 features and utilized two EEG channels. In [35], the authors used
132 a combination of the SVM and RBF to identify drowsiness based on EEG power spectral
133 bands. Nissimagoudar and Nandi [36] described an EEG detection system using an SVM
134 classifier. They detailed an extended driver assistant designed to increase performance and
135 driving safety. A classification result was obtained, ranging from 74 to 89%.

136 All these studies used various classification methods to analyze EEG signals to detect
137 drowsiness phases. Among these, the SVM [37–39] appeared to be the most powerful
138 classification technique. The SVM was developed as a high-performance binary classifier
139 for drowsiness. In addition, this algorithm would allow the implementation of lower Vap-
140 nik–Chervonenkis dimensional architectures. High-dimensional data could then be classified
141 using a lower number of optimization parameters. Thus, these algorithms could solve con-
142 vex optimization problems, which would result in a globally optimal solution. Indeed, this
143 differed from artificial neural networks, which would frequently converge to local minima
144 rather than global minima.

145 To improve classification performance, it is essential to carefully select the most useful
146 features from a wide range of dimensions. In this sense, several approaches have been sug-
147 gested, such as Principal Component Analysis (PCA), Kernel PCA (KPCA), and Independent
148 Component Analysis (ICA). For instance, in [40], the authors compared the PCA, KPCA, and
149 ICA performances for feature extraction as part of the SVM classification. The normalized
150 mean square error was used to compare the performance of the three methods. The result of
151 dimension reduction using KPCA was the most promising, with a strong nonlinear process-
152 ing capability. Similarly, in [41], the authors evaluated two approaches: transfer component
153 analysis and KPCA. They also concluded that KPCA provided the best performance. This can
154 be explained by the fact that EEG data, which always contain a lot of noise, will be denoised
155 by KPCA when transferring common components from the source to the target domain. In
156 [42], the authors combined KPCA and SVM (KPCA-SVM) to detect driving mental fatigue.
157 Their results, with 81.64% accuracy, demonstrated that the KPCA-SVM algorithm increased
158 the generalization capability of the classifier and enhanced the accuracy of recognition of
159 mental fatigue states compared to the PCA-SVM and SVM without feature quality reduction.
160 Accordingly, we have opted for using the KPCA method combined with the SVM to perform
161 drowsiness classification by looking for a minimum feature set.

162 Thus and taking into account all that we have just exposed in the previous part., we
163 propose in the following a drowsiness recognition method based on a combination of TQWT

for EEG-parameter extraction, the KPCA method for feature reduction, and two different machine learning techniques to achieve effective recognition. The main challenge of this work is to develop a new architecture that can be used as a solution for real-time drowsiness detection with the best quality/complexity ratio. The proposed solution must be adapted for an embedded device that can be integrated in the passenger compartment of a car. Thus, the contributions of this study are as follows:

- The creation of a database dedicated to drowsiness analysis and classification is based on EEG signals labelled by an expert doctor.
- The extraction of EEG sub-bands using the TQWT method, where the most appropriate decomposition levels and the best sub-bands are used to eliminate interpersonal problems.
- The identification and selection of the best characteristics for drowsiness recognition using the KPCA method on a minimum feature set.
- The comparative use of two machine learning techniques, SVM and KNN, for drowsiness recognition, where validation is carried out by adopting two strategies: inter-subject and intra-subject. This choice has been motivated by the results reported in the literature on the one hand and by their lower algorithmic complexity on the other hand.
- The minimization of the number of electrodes by identifying the best ones (among the 19 available) to provide the most relevant data reflecting the state of drowsiness.

The remainder of this paper is organized as follows: Sect. 2, while having EEG as the source parameter to effectively predict the vigilance states of a subject, will describe the pre-processing phases applicable to EEG signals and the architectures of the proposed machine learning models which will improve the recognition performance. Section 3 presents the parameters and methods used to validate the proposed system. Finally, we present the experimental setup and a comparative evaluation of the results obtained using the suggested approach.

2 Materials and Methods

2.1 Materials

Existing databases, built with EEG signals collected at home or in controlled environments, focus on the waking stage and various sleep stages [43]. Hypo vigilance, however, is not a fully-fledged state, but a transition between the two stages. This transition, the intermediate point between wakefulness and sleep, is not a subject of interest for experts in the identification of stages. Therefore, it is necessary to build our own database assisted by experts.

In this study, we use EEG database collected from healthy students in our team [13]. These EEG signals are measured at the Vigilance and Sleep Center of the Faculty of Medicine in Monastir with adopting an experimental protocol approved by the Ethics Committee of our faculty. All participants in this database collection signed an informed consent form before starting the experiment. The consent document included a brief description of this research involving human subjects. This database is now available for the moment on request from the corresponding author after upon request. Concerning the anonymisation process of the database we have adopted a common approach of simply removing data fields that contain personal information (name, first name, date of birth, social security number,) which are replaced by a numerical identifier.

This database includes 45 h of data collected from eight subjects between the ages of 21 and 25, which are implicated in drowsiness. Healthy students, with no history of alcoholism

208 or drug use, get up before 10:00 a.m. and take about four hours to complete the task. Each
 209 subject's record is represented by 19 EEG derivations, which are shown in Fig. 1. This last one
 210 represents original trace of a patient belonging to our database recorded during a transition
 211 between wakefulness and sleep.

212 The common electrodes in all recordings are four EEG channels, two central zones (C3
 213 and C4), and two occipital zones (O1 and O2), each of which is acquired at 500 samples
 214 per second. The positions of the electrodes are shown in Fig. 2. The EEG signals are filtered
 215 using a 2nd order band-pass Butterworth filter between 0.5 and 50 Hz.

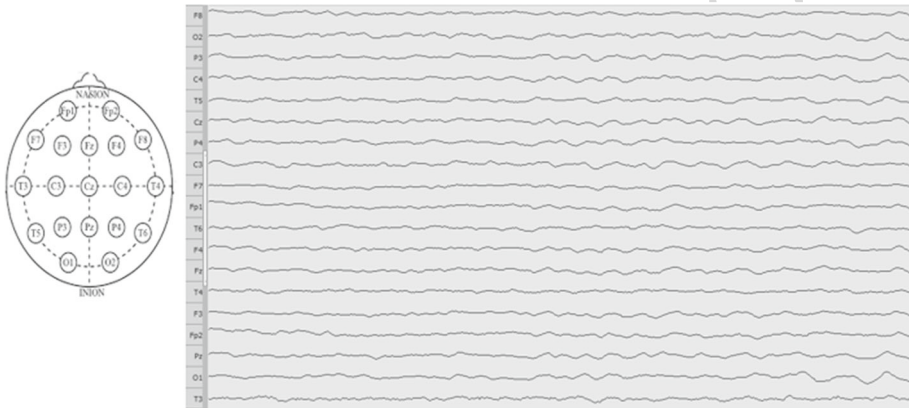


Fig. 1 Original 10-s record of a patient taken during the awake-sleep transition phase

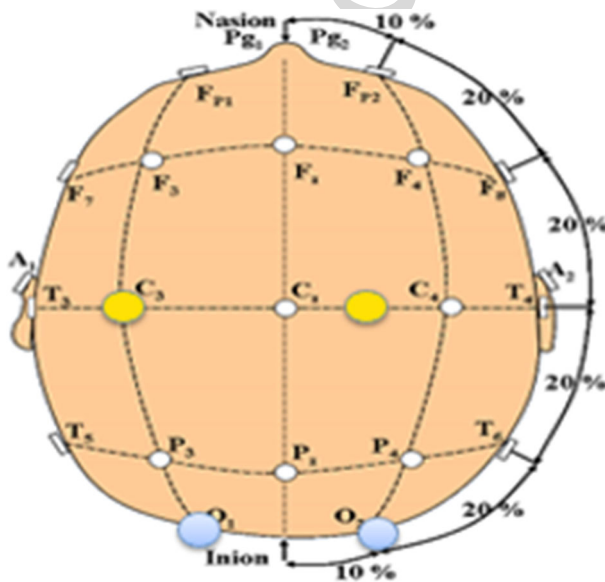


Fig. 2 Distribution of electrodes. All recordings used four EEG channels, two central zones (C3 and C4 in yellow) and two occipital zones (O1 and O2 in light blue)

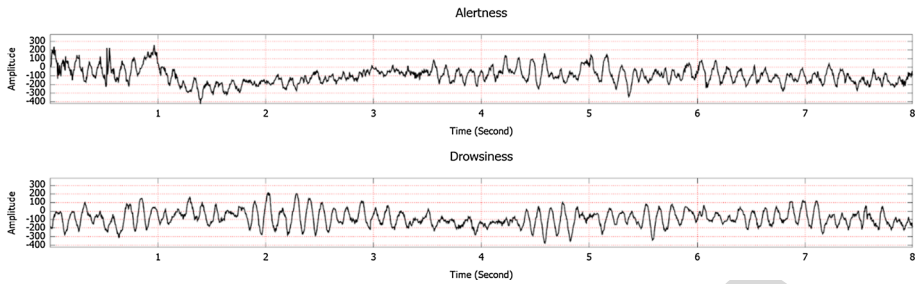


Fig. 3 EEG signal tracing and labels based on expert assistance for three mental states: **a** alertness and **b** drowsiness

216 The labelling of the different vigilance levels is carried out manually by an expert in
 217 EEG and polysomnography. The expert classified these recordings at intervals of 10 s and
 218 30 s. These intervals are sufficiently large to guarantee precise drowsiness state detection
 219 sufficiently early. For each subject, the expert adopts two labels corresponding to two states
 220 of vigilance: alertness and drowsiness (Fig. 3).

221 To make the EEG signal efficiently usable in the extraction and classification phase without
 222 causing the inter-individual variation problem, a time segmentation phase followed by a
 223 normalization phase is required. Thus, time segmentation of the input data is performed at
 224 intervals of 10-s. Indeed, increasing the time segment improves the accuracy of the proposed
 225 system. For this reason, the 10-s window elapses one second for each treatment, and the system
 226 should therefore give a result every second. Thereafter, the EEG signals are normalized by
 227 converting the values to z-scores. Z scores are expressed in terms of standard deviations from
 228 their mean. Thus, the scores of the different distributions can be directly compared [44].

229 All calculations in this work have been run on an Intel (R) Core™i3-4005U, 1.70 GHz
 230 CPU with 8 GB of RAM. The experiments have used MATLAB version R2015a.

231 2.2 Drowsiness Recognition Using EEG Analysis

232 As mentioned in the introduction, one of the most important approaches to estimating vigi-
 233 lance is the use of physiological measurements. EEG is a precious and cost-effective signal
 234 used to assess the electrical activity of the brain. EEG has a non-invasive appearance and is
 235 dynamic, stochastic, non-linear, and non-stationary, with a small amplitude. Generally, EEG
 236 signals are widely regarded as reliable measures of drowsiness, fatigue, and performance
 237 assessment [2].

238 Characteristics based on Power Spectral Density (PSD) are the most widely used for EEG-
 239 based drowsiness surveys [8]. The decrease in arousal is characterized by slowing down and
 240 desynchronization of cortical electrical activity. EEG bands can be represented as low-and
 241 high-frequency activities. Figure 4 illustrates five traditional EEG frequency bands: delta δ
 242 (0.1–4 Hz), theta θ (4–8 Hz), alpha α (8–13 Hz), beta β (13–30 Hz), and gamma γ (30–50 Hz).
 243 The frequency band distribution changes over time, and the occurrence of frequency bands
 244 can be used as a feature related to the drowsiness state.

245 The low-frequency bands, in particular the α band, show increased power during the
 246 drowsy phase compared to the alert phase. Drowsiness leads to increased α and θ activi-
 247 ties with eyes open, while α decreases and θ increases with eyes closed [45]. Indeed, α
 248 is predominant when the person is alert. When they close their eyes, α is gradually replaced

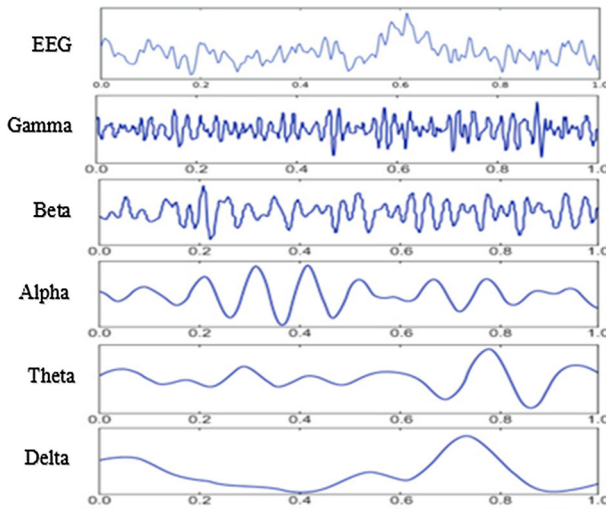


Fig. 4 Representations of most popular EEG frequency bands. Five traditional EEG frequency bands, including Delta δ (0.1–4 Hz), Theta θ (4–8 Hz), Alpha α (8–13 Hz), Beta β (13–30 Hz), and Gamma γ (30–50 Hz)

249 by a θ activity with increasing drowsiness. The α activity, which decreases in the occipital
 250 regions, sometimes increases in the central and frontal regions with fatigue [46]. The θ
 251 activity increases mainly in the frontal and central regions [46].

252 The high-frequency EEG bands (β and γ), in particular the beta band, show a reduction
 253 in the power of the band throughout drowsiness [46]. In terms of brain regions, the frontal,
 254 parietal, and occipital regions are suggestive; in particular, the α activity of the occipital region
 255 and the β of the frontal region are two potential indicators. Thus, finding informational brain
 256 regions with particular frequency bands will reduce the number of electrodes needed to
 257 develop an effective EEG-based drowsiness detection and warning system.

258 2.3 Proposed Method and Process of Experiment

259 The approach is proposed to differentiate between alertness and drowsiness, so the detec-
 260 tion of hypo-vigilance consists of two main steps: the extraction of characteristics from the
 261 EEG signals and their classification. Figure 5 shows the operations performed, from EEG
 262 sampling to hypo vigilance detection. Initially, the segments marking the awake and drowsy
 263 phases are taken from the dataset. Then, the data are segmented into 10-s elapsed windows,
 264 produced every second. Subsequently, the data are normalized using Z-score. The result of
 265 the normalization of each segment is decomposed into sub-bands using TQWT. From these
 266 sub-bands, the alpha and theta bands are used to extract the features and KPCA to identify
 267 highly discriminating features. Finally, these features are fed to the SVM to determine their
 268 classes.

269 2.3.1 Extraction and Feature Selection

270 **Tunable Q-Factor Wavelet Transform** The feature extraction process requires the applica-
 271 tion of a denoising algorithm (to remove artifacts) and dimensionality reduction (to speed up

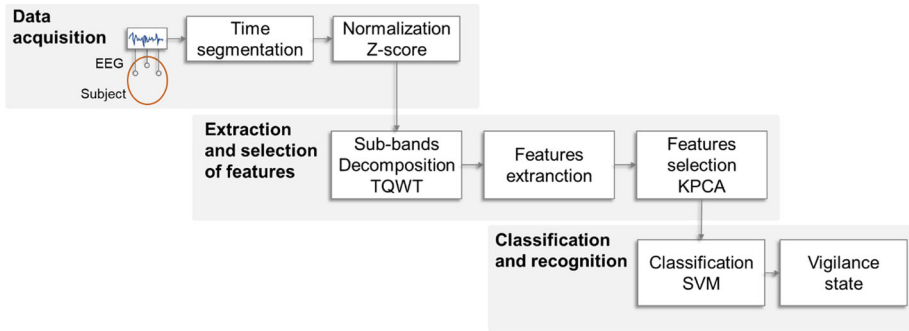


Fig. 5 Operations performed from EEG sampling to hypo vigilance detection: Data acquisition (production of 10-s windows and Z-score normalization), feature extraction (decomposition in sub-bands and identification of highly discriminating features using KPCA) and classification using SVM

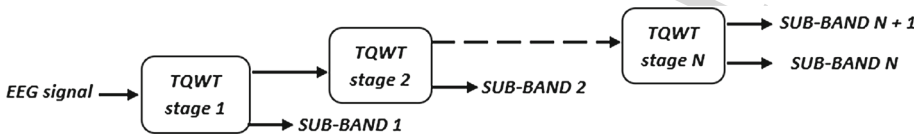


Fig. 6 TQWT based decomposition level of input signal. The input values are broken down into $N + 1$ low-pass and high-pass sub-bands, where N is the number of stages of the two banks of channel filters

the identification process). Therefore, instead of using a Discrete Wavelet Transform (DWT) to capture both frequency and location in time, we use a TQWT. Indeed, the TQWT allows adjustable parameters and a very fast response time [22]. Additionally, the TQWT is proposed to provide an efficient and distributed representation of the oscillatory signals.

The TQWT is characterized by three parameters: Q-factor, redundancy r , and the number of levels of decomposition J . The parameter Q defines the number of oscillations of the wavelet, and r defines the frequency overlap. The input values are broken down into $N + 1$ low-pass and high-pass sub-bands, where N is the number of stages of the two banks of the channel filters. For more details on the TQWT, the authors explained in [47] the choice of the parameters and the influence of each parameter as regards the performance of the adopted solution. According to the trade-off between processing speed and precision, the resulting chosen parameters are $Q = 1$, $r = 3$, and $j = 7$.

The TQWT consists of a sequence of dual-channel filter banks, and the low-pass output of each filter bank is used as the input for successive filter banks. Each output signal is a wavelet-transform sub-band. The decomposition of the signal into $N + 1$ sub-bands is shown in Fig. 6.

In our case, we process the sub-bands expressing the α and θ activities. The sub-bands expressing the α and θ activities are sub-bands 5 and 6. We are interested in temporal and frequency features that represent both activities. Three features are extracted based on the frequency domain and nine features are extracted from the temporal domain for distinguishing 'Alert' and 'Drowsy' EEG epochs. These features are illustrated in Fig. 7.

Kernel Principal Component Analysis As a pre-processing method, KPCA proves helpful for classification [48]. As a feature extractor, the features pre-treated by KPCA have smaller

Frequency features	Temporal features (Alpha band)	Temporal features (Theta band)
F.1 Alpha band power / Theta band power	T.1 Activity: Hjorth params [44,45]	T.10 Activity: Hjorth params [44,45]
F.2 Alpha band power / Total band power	T.2 Mobility: Hjorth params [44,45]	T.11 Mobility: Hjorth params [44,45]
F.3 Theta band power / Total band power	T.3 Complexity: Hjorth params [44,45]	T.12 Complexity: Hjorth params [44,45]
	T.4 Mean	T.13 Mean
	T.5 Standard deviation	T.14 Standard deviation
	T.6 Skewness	T.15 Skewness
	T.7 Kurtosis	T.16 Kurtosis
	T.8 Root mean square RMS	T.17 Root mean square RMS
	T.9 Entropy [46]	T.18 Entropy [46]

Fig. 7 Frequency and time domain features extracted from EEG signals

295 dimensions, which improves the efficiency of classification. KPCA is an extension of PCA.
 296 It is a technique that generalizes linear PCA for nonlinear cases using the kernel method.
 297 Given the high size and non-linearity of the EEG signal, the kernel method is a powerful tool
 298 for the classification of this type of signal.

299 KPCA performs a nonlinear form of PCA with integral operator kernel functions $\Phi(x)$
 300 [48], considering that the data x_i , with $i = 1, 2, \dots, N$ and $x_i \in R^N$ are represented in the feature
 301 space K by:

$$\begin{aligned} \Phi : R^N &\rightarrow K \\ x_i &\rightarrow \Phi(x_i) \end{aligned} \quad (1)$$

302 Let us first assume that our projected features have zero-average as follows:

$$\frac{1}{N} \sum_{i=1}^N \Phi(x_i) = 0 \quad (2)$$

303 The covariance of the projected new features is calculated by:

$$C = \frac{1}{N} \sum_{i=1}^N \Phi(x_i) \Phi(x_i)^T \quad (3)$$

304 The eigenvectors and eigenvalues of this covariance matrix are:

$$C V_k = \lambda_k V_k \quad (4)$$

305 with $k = 1, 2, \dots, D$ and D are the dimensions of the data mapped into the K -space.
 Using (3) and (4), we have:

$$C V_k = \frac{1}{N} \sum_{i=1}^N \Phi(x_i) \Phi(x_i)^T V_k = \lambda_k V_k \quad (5)$$

306 This can be reworded as follows:

$$V_k = \frac{1}{N} \sum_{i=1}^N a_i \Phi(x_i) \quad (6)$$

321 If we replace V_k in Eq. 5 with Eq. 6, we obtain:

$$322 \quad CV_k = \frac{1}{N} \sum_{i=1}^N \Phi(x_i) \Phi(x_i)^T \sum_{j=1}^N a_j \Phi(x_j) = \lambda_k \sum_{i=1}^N a_i \Phi(x_i) \quad (7)$$

324 The kernel function is set:

$$325 \quad K(x_i, x_j) = \Phi(x_i)^T \Phi(x_j) \quad (8)$$

327 If we multiply both sides of Eq. 7 by $\Phi(x_i)^T$, we obtain:

$$328 \quad \frac{1}{N} \sum_{i=1}^N K(x_i, x_j) \sum_{j=1}^N a_j K(x_i, x_j) = \lambda_k \sum_{i=1}^N a_i K(x_i, x_j) \quad (9)$$

330 We apply the matrix notation as follows:

$$332 \quad K^2 A_k = \lambda_k N K A_k \quad (10)$$

333 with $K_{i,j} = K(x_i, x_j)$.

334 The resulting kernel principal components are given by:

$$336 \quad y_k(x) = \Phi(x)^T V_k = \sum_{i=1}^N a_i K(x, x_i) \quad (11)$$

337 It is essential to have zero mean in the kernel space. If the data in the kernel space do
338 not have a zero mean, we use the Gram \tilde{K} matrix to replace our kernel matrix K . The Gram
339 matrix \tilde{K} is given by:

$$340 \quad \tilde{K} = K - 1_N K - K 1_N + 1_N K 1_N \quad (12)$$

342 where 1_N is an $N \times N$ matrix and all elements are equal to $1/N$.

343 In our case, the Gaussian function was selected as the kernel function for the KPCA
344 algorithm. This function is defined as follows:

$$346 \quad K_{\sigma}^{Gaussian}(x, y) = \exp\left(\frac{\|x - y\|^2}{\sigma^2}\right) \quad (13)$$

347 where σ is the width of the Gaussian kernel.

348 **Classification Using Support Vector Machine** SVM, which is a machine learning algorithm,
349 is a powerful tool for brain-computer interface (BCI) applications for real-time EEG classifi-
350 cation [30]. It aims to search the hyperplane not only to obtain a better classification based on
351 support vectors, but also to maximize the geometric margin in the classification (Fig. 8). This
352 approach maximizes the margin, which is the closest distance between two corresponding
353 samples in each separate class (the alert and drowsy classes). For margin maximization, the
354 mathematical model of the SVM is presented in Eq. 14:

$$355 \quad \min \frac{1}{2} \|w\|^2 + C \sum_{i=1}^n \xi_i$$

$$358 \quad \text{s.t. } y_i(w, x_i) + b \geq 1 - \xi_i, \xi_i \geq 0, \quad i = 1, 2, \dots, n \quad (14)$$

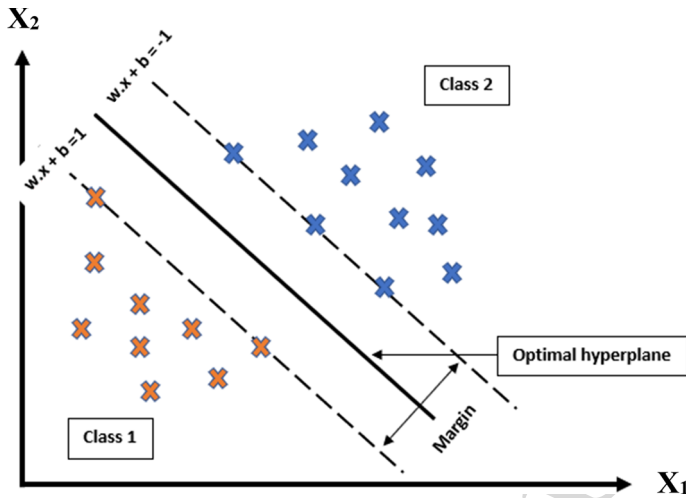


Fig. 8 SVM classifier

where x_i is a set of given training vectors with $x_i \in R^n$, y_i is the corresponding label of x_i , w is the normal weight vector to the hyperplane, b is the bias, ξ_i is a slack variable, and C is a penalty factor.

Using the SVM, the system can match the predictor data to the hyperplane, and kernel functions can successfully perform both linear and nonlinear classification [49]. In this context, the RBF is the most popular of all SVM kernels. This kernel is mathematically defined by Eq. 15:

$$K(x_i, x) = \exp(-\gamma \|x_i - x\|^2), \gamma > 0 \quad (15)$$

where $K(x_i, x)$ is the kernel function, which is based on the internal product of the two variants x_i and x , and γ defines the scope of the impact of a single learning example.

The RBF kernel is tuned for two parameters: the penalty factor C , which balances the relative importance of minimizing the learning error and maximizing the class margins, and the γ parameter, which defines the degree of similarity between points [50].

Overview of Proposed TQWT-KPCA Model Our suggested TQWT-KPCA procedure and associated parameters, shown in Fig. 9, can be summarized as follows:

- Step 1. Data pre-processing (filtering, normalization and segmentation).
- Step 2. Division of EEG segment into sub-bands using TQWT.
- Step 3. Features extraction.
- Step 3. Perform KPCA for features selection.
- Step 4. Use SVM to predict "alert or drowsy" driver state.

3 Validation and Testing

Different metrics are applied in this study to evaluate the performance of the proposed approach. For this purpose, three metrics are used: accuracy, specificity, and sensitivity.

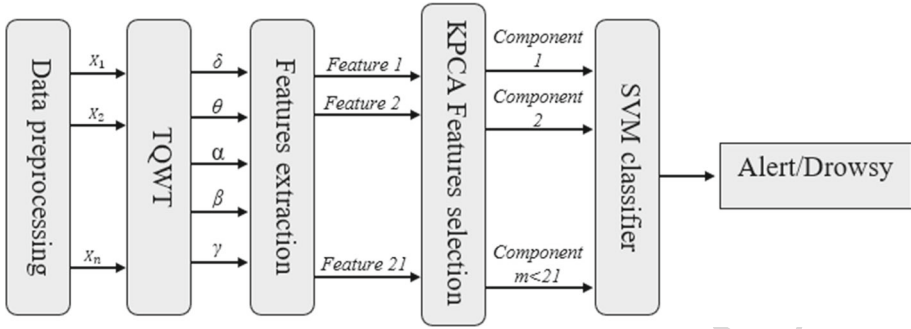


Fig. 9 Procedure of TQWT-KPCA model

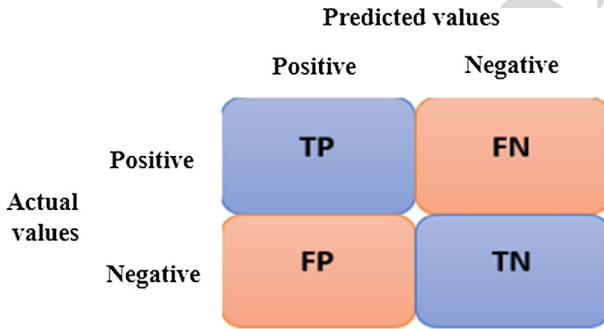


Fig. 10 Confusion matrix. Correlation between actual and predicted values in the form of (TP), (FP), (TN) and (FN) results

382 These metrics are computed using a tenfold cross-validation strategy [51]. This strategy is
 383 based on the information obtained from the confusion matrix illustrated in Fig. 10, where
 384 four results are provided.

- 385 True Positive (TP): prediction of drowsiness when the actual state is drowsiness.
- 386 False Positive (FP): prediction of drowsiness when the actual state is alertness.
- 387 True Negative (TN): prediction of alertness when the actual state is alertness.
- 388 False Negative (FN): prediction of alertness when the actual state is drowsiness.

389 The performance measurement parameters (precision, sensitivity, and specificity) were
 390 computed as follows:

$$392 \text{ Accuracy} = \frac{TP + TN}{TP + FP + TN + FN} \tag{16}$$

$$393 \text{ Specificity} = \frac{TN}{TN + FP} \tag{17}$$

$$394 \text{ Sensitivity} = \frac{TP}{TP + FN} \tag{18}$$

397 The training and test datasets are divided by subject so that three randomly selected
 398 subjects are used for training and testing, and the remaining five subjects are only utilized
 399 for testing. Specifically, the samples of three subjects are divided into 70% for training and

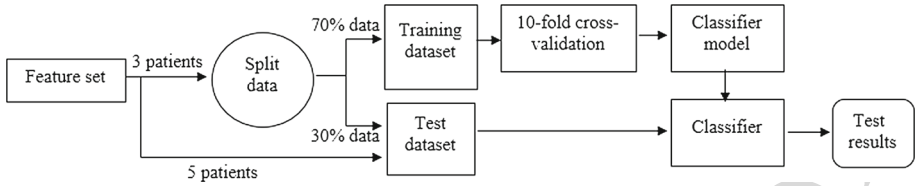


Fig. 11 Organization of data for classifier training and testing

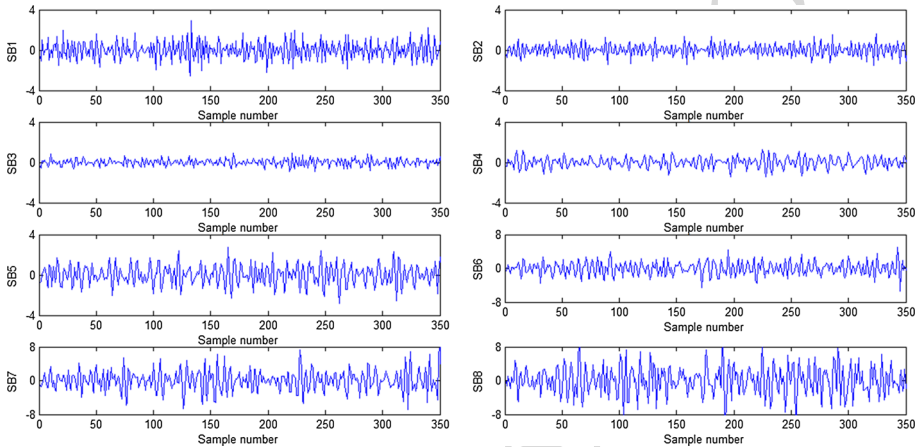


Fig. 12 Sub-bands using TQWT decomposition

400 30% for testing, and the samples of the remaining subjects are used for testing, as shown in
 401 Fig. 11.

402 4 Results and Discussion

403 4.1 Results

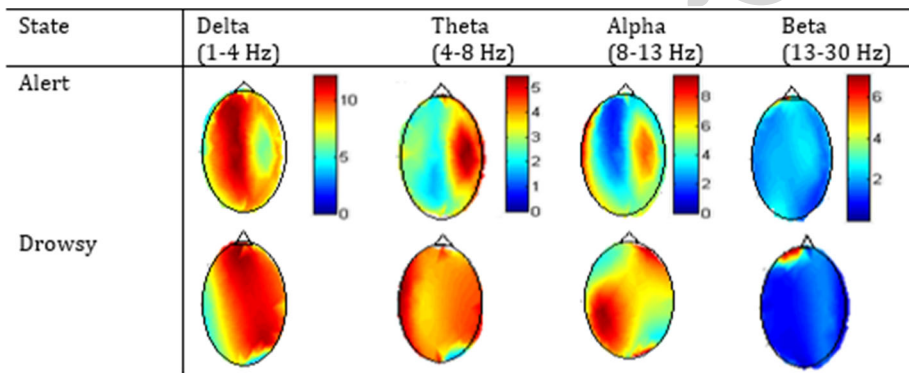
404 4.1.1 Inter-subject Results

405 **Extraction Sub-bands Using TQWT** The sub-bands are obtained by transforming the EEG
 406 signals into a different domain, as mentioned in Sect. 2.3.1.1. Among the existing methods of
 407 transformation of the time–frequency domain, the TQWT is applied to obtain the sub-bands.
 408 It can cover the frequency ranges of the required sub-bands and recover the time-domain
 409 signal with very little waste. Figure 12 shows an example of EEG signal decomposition at
 410 the J level using the TQWT.

411 Regarding the choice of sub-bands from which the different characteristics will be
 412 extracted, we explore the variation in the mean frequency of the EEG during alert and drowsy
 413 states. The mean frequency of the EEG signals provides an indicator of the general slowing
 414 down of brain activity. Table 1 shows the average frequency of each band for all the patients.

Table 1 Mean frequency of EEG in different spectral bands (sub-bands) for states of alert and drowsiness

State	Delta (1–4 Hz)	Theta (4–8 Hz)	Alpha (8–13 Hz)	Beta (13–30 Hz)	Gamma (30–50 Hz)
Alert	2.29	5.47	9.98	23.68	38.22
Drowsy	2.27	6.03	9.65	23.51	38.15
Difference	0.02	– 0.56	0.33	0.17	0.07
Difference %	1%	– 10%	3%	1%	0%

**Fig. 13** Scalp topography for each spectral band (delta, theta, alpha, beta)

415 Furthermore, the mean frequency of the alert state is almost equal to that of the drowsy state,
 416 except for the theta (difference: -0.56 Hz) and alpha (difference: 0.33 Hz) bands.

417 Our approach consists in splitting the EEG signal into five sub-bands using TQWT. Thus,
 418 we obtain 95 sub-bands (5 sub-bands \times 19 electrodes) for each segment of 10 s. For each
 419 sub-band, we calculate 21 features, so that we have as a general result for the entire segment
 420 $95 * 21 = 1995$ features.

421 Topographical analysis is required to locate the most appropriate electrodes that reflect
 422 the best variation corresponding to the wake-sleep transition. The scalp topographies indicate
 423 that when the spectral band or brain region is changed, the amplitude also changes. Figure 13
 424 depicts the scalp topographies for the different EEG spectral bands for all recordings with
 425 19 electrodes. The scalp topographies represent the mean power band used to show brain
 426 activity during the wake-sleep transition. The amplitude is calculated for every EEG channel
 427 and the frequency band. Furthermore, an increase in theta and alpha power amplitudes in the
 428 central and occipital regions is observed during drowsiness compared to vigilance. However,
 429 in both the delta and beta bands, there are no significant differences in amplitude variations.
 430 Furthermore, an increase in the theta and alpha power amplitudes in the central and occipital
 431 regions is noticed during drowsiness compared to vigilance. Utilizing these features, we can
 432 conclude that the useful information of our system is mainly focused on the central and
 433 occipital regions. Moreover, we note that the variations during drowsiness are located mainly
 434 in the central and occipital regions. Based on these interpretations, we decide to work only
 435 on the alpha and theta sub-bands using the bipolar channel C3-O1.

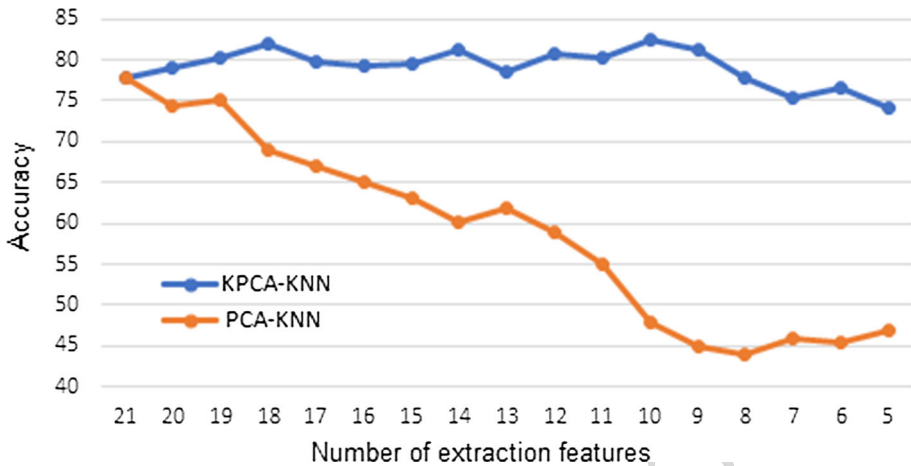


Fig. 14 Relation between classification accuracy and number of features for KPCA-KNN and PCA-KNN algorithms. The maximum accuracy of 82.39% for the KPCA-KNN obtained using 10 features

436 **Reduction Features Using PCA, KPCA and the KNN Classifier** We test the KNN algorithm
 437 for the advanced validation of the proposed classifier. We utilize the same testing feature set
 438 as the SVM.

439 The KNN is a memory-based, non-parametric classification method that does not require
 440 a model inclusion in data and uses observations from the training set to identify the most
 441 similar properties. The only parameter in this algorithm is K , which is the number of nearest
 442 neighbour's to be considered. Here, $K = 3$ is chosen. In addition, the Euclidean distance
 443 function is employed using an "inverse squared" distance weight [27]. The results of the test
 444 sessions are shown in Fig. 14. By varying the number of features, we obtain a maximum
 445 accuracy of 82.39% using 10 features.

446 **Reduction Features Using PCA, KPCA and SVM Classifier** Input features are fundamental
 447 to the classification efficiency. After determining the features to be used as an input vector,
 448 we proceed to the selection of a classifier capable of improving the ability to identify the
 449 transitions between drowsy and alert states from EEG signals.

450 In this study, RBF-SVM is generated utilizing various values of C and γ parameters.
 451 These parameters are tested in the range $[0.1-10]$ and selected because they offer the highest
 452 accuracy. The best results were obtained by setting C to 1.0 and γ to 0.4 ((best accuracy is
 453 89% in Fig. 15). To differentiate between alertness and drowsiness states, after extracting
 454 the parameters from our EEG signal, the KPCA-SVM is applied. Classification accuracy is
 455 observed based on the number of parameters extracted using KPCA and PCA. The average
 456 classification accuracy is shown in Fig. 16.

457 Figure 16 illustrates the extent to which a change in the selection of the number of features
 458 can affect the classification accuracy. The accuracy varies with the number of features. When
 459 the number of features is higher than 10, the accuracy of the classification is greater than
 460 84%. The maximal classification accuracy, 89%, is achieved when the number of element
 461 dimensions is 12. In addition, the performance of the KPCA-SVM significantly exceeds that
 462 of the PCA-SVM.

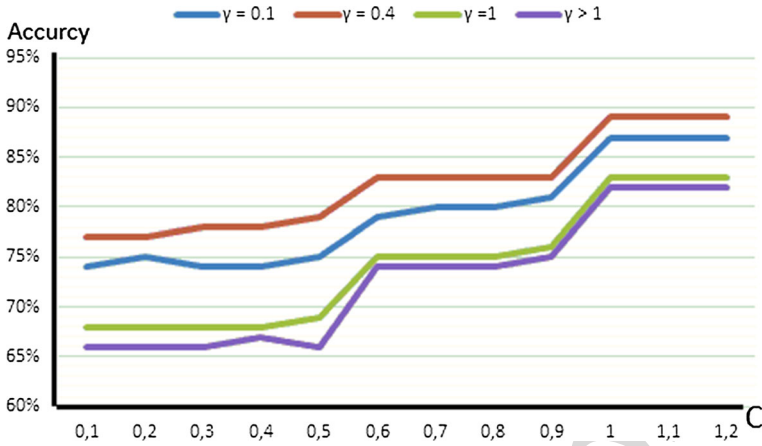


Fig. 15 Accuracy variation for different values of C and γ

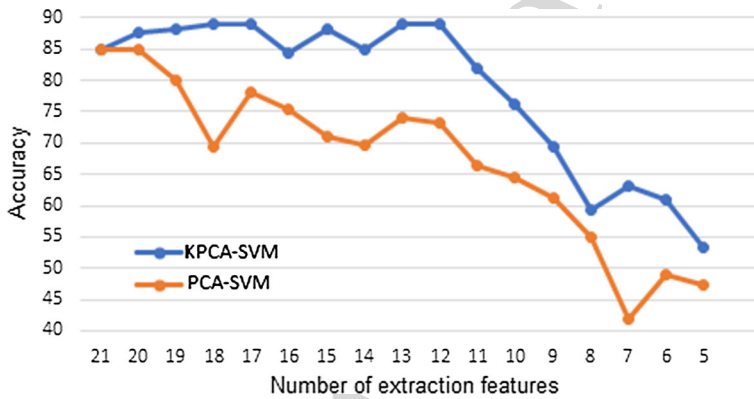


Fig. 16 Relation between classification accuracy and number of features for KPCA-SVM and PCA-SVM algorithms. The maximum accuracy of 89% is obtained with KPCA-SVM using 12 features

463 The maximum accuracy obtained by varying the number of features using the SVM classifier is 89%.
 464 On the other hand, the maximal accuracy obtained with the same methodology
 465 using the KNN classifier is 82.39%. Based on these two results, it is found that the SVM
 466 classifier is preferable to the KNN classifier.

467 **Receiver-Operating Characteristics Using KPCA** KPCA is used to determine the minimum
 468 number of features that achieved a good accuracy. Figure 17 summarizes the receiver operating
 469 characteristic (ROC) results for different numbers of features. Twelve is the minimum
 470 number of features that provide the best result for differentiation between the two stages.
 471 It provides an accuracy rate of 89.37% for drowsiness detection and 88.07% for vigilance
 472 detection.

473 The experimental results show that, with our database, for efficient classification, properly
 474 selected features are necessary. The graphs in Fig. 18 show the efficiency of the KPCA-
 475 SVM algorithm in terms of sensitivity, specificity, and classification accuracy with different

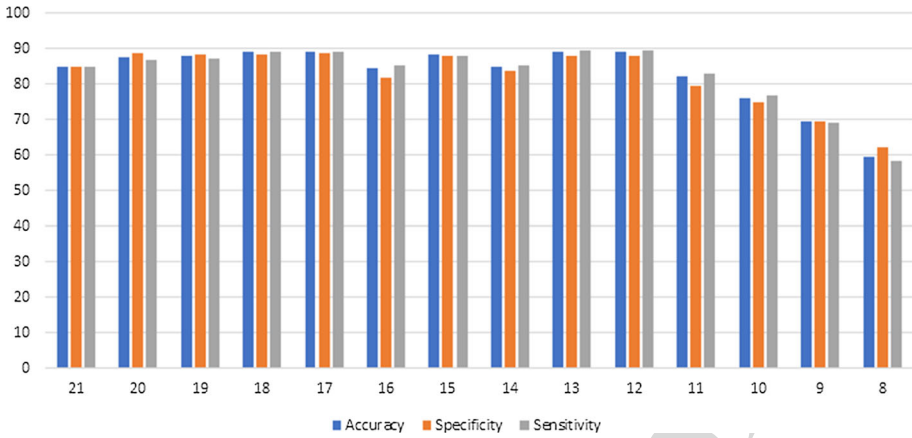


Fig. 17 Average result of ROC parameters for different numbers of features

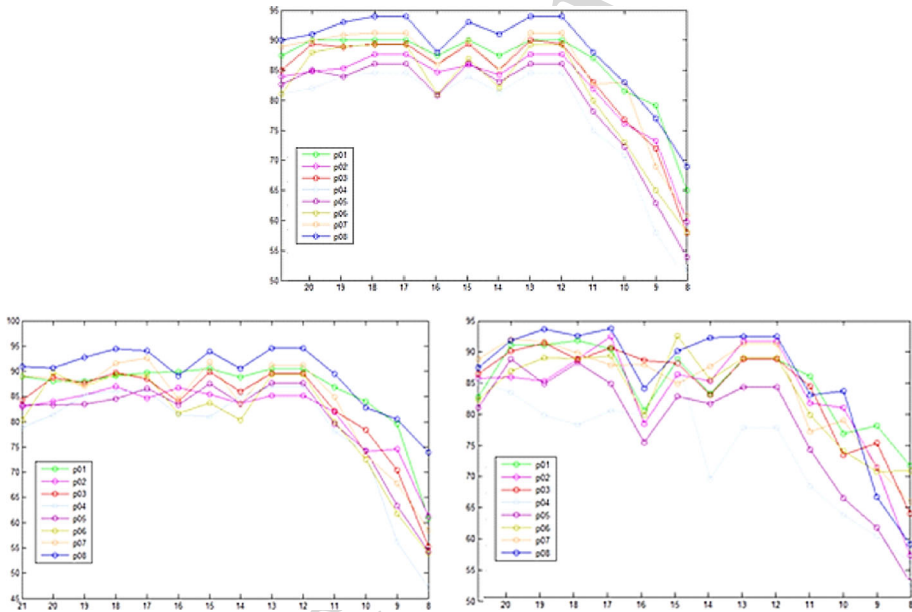


Fig. 18 Performance evaluation according to number of features selected for each person: **a** sensitivity, **b** specificity and **c** accuracy

476 numbers of principal components for each patient in the database used in the test. These
 477 graphs are obtained using KPCA with an RBF-SVM classifier. From the results given in
 478 Fig. 18, it is clear that the proposed algorithm works effectively for all the patients tested. We
 479 have obtained the best rates in the measures used to evaluate the performance of the proposed
 480 work. For most of the patients, we obtain a maximum rate in terms of accuracy, specificity
 481 and sensitivity, when the number of principal components extracted by KPCA is around 12.

482 Once the number of extracted principal components is less than 12, the performance of the
483 classifier for all patients starts to decrease.

484 4.1.2 Intra-subject Results

485 To ensure the effectiveness of our system, we also apply our system per person, such that
486 for each subject, we take 70% of the recording for training and 30% for testing. The average
487 result for all the subjects is approximately 94%.

488 4.2 Discussion

489 The intra- and inter-subject variability of EEG has hampered the development and application
490 of drowsiness detection systems. The choice of features is always the most important step in
491 the detection of decreased alertness. Adding the issue of interpersonal variability and driver
492 comfort, this step becomes a challenge. The TQWT is used to divide the signal in sub-bands.
493 Then the choice of features allows the interpersonal variability problem to be overcome
494 without compromising the accuracy of 85%. The use of single-channel EEG makes the
495 system convenient for drivers and is more suitable for the development of real-time systems.
496 Furthermore, by removing unnecessary and redundant features, the efficiency and generality
497 of the system's classification is enhanced, which explains the shift from the accuracy of
498 approximately 85% using all features (21 features) to 89% using only 12 features. Utilizing
499 the KPCA algorithm, the accuracy of the classification is further increased to approximately
500 89%, and the system becomes faster by reducing the number of features from 21 to 12.

501 This study can be used as a step in the development of a drowsiness monitoring device
502 based on EEG signals. Several studies have pointed to the possibility of detecting driver
503 drowsiness from EEG signals. In Table 2, we compare our approach with existing methods
504 that use the process results for the combined subjects. In [8], the authors used 19 features
505 using DWT and FFT to estimate an individual's drowsiness with an accuracy of 87%. The
506 authors of [52] presented a system based on features obtained from the alpha band and an
507 MLP classifier, and an accuracy rate of 88% was achieved.

508 Since most studies have not taken into account interpersonal problems and have not tested
509 their system per person, we add another table (Table 3), which compares the results obtained
510 by applying our system per person with the results using the same strategy. However, the
511 authors in [13] used the same database as ours, and the result obtained was approximately 10%
512 lower than our classification accuracy. In [55], the authors proposed drowsiness detection
513 using eight features extracted from EEG signals and an SVM for classification, and an
514 accuracy rate of 83% was obtained.

515 This large difference in terms of performance is mainly due to:

- 516 • The use of a 1 s sliding window in the EEG signal. This technique allows the signal to be
517 analyzed by fractions assumed to be stationary. This approach is rather original compared
518 to other studies mentioned in Tables 2 and 3, which used EEG portions of fixed widths
519 ranging between 10 and 30 s. Thus, these sliding windows make it possible to detect rapid
520 transitions in brain activity, in our case drowsiness.
- 521 • The large number of EEG signal derivations used in most bibliographic studies. Indeed,
522 the authors in these articles used a rather high number of inputs. As we have already noted
523 in our article we have used only one derivation which is the (C3-O1) with those two alpha
524 and theta bands that best characterize the drowsiness phase. (Sect. 4.1.1.1).

Table 2 Comparison of proposed method with other systems: generic solutions

Reference	Pre-process methods	Classifier model	Time window	Signal sources	Accuracy	Specificity	Sensitivity
[8]	DWT, FFT	ANN	10 s	MIT-BIH Polysomnographic	87.40%	–	–
[53]	BPF	DNN	30 s	MIT-BIH Polysomnographic	85.01%	84.57%	88.02%
[52]	FFT	ANN	30 s	MIT-BIH Polysomnographic	88%	85.04%	88.55%
[54]	DWT	ANN	10 s	MIT-BIH Polysomnographic	86.5%	–	–
Proposed method	TQWT-KPCA	SVM	10 s [1 s]	Sahloul University Hospital	89%	88.07%	89.37%

Table 3 Comparison of proposed method with other systems: personalized solutions

Reference	Pre-process methods	Classifier model	Time window	Signal sources	Accuracy	Specificity	Sensitivity
[22]	TQWT	ELM	-	MIT-BIH Polysomnographic	91.8%	85.4%	96.5%
[13]	-	DL	-	Sahloul University Hospital	85%	-	-
[56]	KPCA	SVM	10 s	-	85%	83%	84%
[57]	Mutimodel	SVM	30 s	MIT-BIH Polysomnographic and YAWDD	87.2%	-	-
[58]	PSD	SWLDA- SVM	10 s	-	72.7%	45.2%	88.7%
[59]	FFT	RF	10 s	-	81.4%	84.8%	-
[60]	FFT	RF	-	Max Planck Institute Leipzig Mind-Brain-Body database	87.00%	88%	86%
[55]	PSD	SVM	-	MIT-BIH Polysomnographic	83.36%	-	-
[61]	FFT	DT	10 s	-	84%	-	86.83%
[62]	CNN	DSTCLN	10 s	-	87%	88%	86%
[63]	wavelet entropy	SVM	-	-	90.7%	-	-
Proposed method	TQWT-KPCA	SVM	10 s [1 s]	Sahloul University Hospital	94%	93.78%	94.08%

- 525 • The TQWT extraction method coupled with the KPCA which allowed reducing the feature
526 number while adapting with the transitory nature of the EEG signal.

527 5 Conclusion

528 Drowsiness precedes sleep or the need to sleep. Drowsiness becomes dangerous if a certain
529 level of concentration is required, for example when driving motor vehicles. In this work,
530 we put forward a drowsiness detection system based on features extracted from a unique
531 EEG channel. Our system is based on the TQWT for EEG signal decomposition, KPCA
532 for feature selection, and SVM for distinguishing between alertness and drowsiness. The
533 suggested approach can detect drowsiness with accuracy of approximately 89% and 94% for
534 inter- and intra-subject systems, respectively.

535 The advantage of our method, in addition to a good rate of detection of hypo vigilance
536 states, is that it can solve the problem of interpersonal variability. Furthermore, our database,
537 specially built for the study of hypo vigilance, is of great help in analyzing the problem
538 properly. Finally, the proposed hypo vigilance detection algorithm, besides to its fast response,
539 robustness and precision, can be applied in real time.

540 In the future, we plan to integrate other physiological signals, like the ECG and the EMG,
541 with EEG signals to improve the robustness of the system. Moreover, hardware integration
542 on embedded devices (FPGA and/or microprocessors) of the proposed approach will be the
543 subject of future work. For example, wireless portable EEG headsets can be used for the
544 acquisition of a limited number of physiological signals in the car passenger compartment
545 (e.g. the EPOC + headset from emotiv¹ or the maindwave from neurosky 2²).

546 References

- 547 1. Kundinger T, Sofra N, Riener A (2020) Assessment of the potential of wrist-worn wearable sensors for
548 driver drowsiness detection. *Sensors* 20(4):1029
- 549 2. Belakhdar I, Kaaniche W, Djmel R, Ouni B (2016) Detecting driver drowsiness based on single electro-
550 encephalography channel. In: 2016 13th international multi-conference on systems, signals & devices
551 (SSD). IEEE, pp 16–21
- 552 3. Zhang C, Wang W, Chen C, Zeng C, Anderson DE, Cheng B (2018) Determination of optimal electroen-
553 cephalography recording locations for detecting drowsy driving. *IET Intel Transport Syst* 12(5):345–350
- 554 4. Doudou M, Bouabdallah A, Berge-Cherfaoui V (2019) Driver drowsiness measurement technologies:
555 current research, market solutions, and challenges. *Int J Intell Transp Syst Res* 18:297–319
- 556 5. Forsman PM, Vila BJ, Short RA, Mott CG, Van Dongen HP (2013) Efficient driver drowsiness detection
557 at moderate levels of drowsiness. *Accid Anal Prev* 50:341–350
- 558 6. McDonald AD, Schwarz C, Lee JD, Brown TL (2012) Real-time detection of drowsiness related lane
559 departures using steering wheel angle. In: Proceedings of the human factors and ergonomics society
560 annual meeting, vol 56, no 1. SAGE Publications, Los Angeles, CA, pp 2201–2205
- 561 7. Sahayadhas A, Sundaraj K, Murugappan M (2012) Detecting driver drowsiness based on sensors: a review.
562 *Sensors* 12(12):16937–16953
- 563 8. Correa AG, Orosco L, Laciari E (2014) Automatic detection of drowsiness in EEG records based on
564 multimodal analysis. *Med Eng Phys* 36(2):244–249
- 565 9. SmartEye (2019) Driver monitoring system. Interior sensing for vehicle integration. [https://smarteeye.se/
566 automotive-solutions/](https://smarteeye.se/automotive-solutions/). Accessed 27 Aug 2020

¹ <https://www.emotiv.com/>.

² <https://store.neurosky.com/>.

- 567 10. Edenborough N, Hammoud R, Harbach A, Ingold A, Kisananin B, Malawey P, Newman T, Scharenbroch
568 G, Skiver S, Smith M, Wilhelm A (2005) Driver state monitor from delphi. In: 2005 IEEE Computer
569 Society conference on computer vision and pattern recognition (CVPR'05), vol 2. IEEE, pp 1206–1207
- 570 11. Optalert (2019) Scientifically validated Glasses-Mining. [https://www.optalert.com/explore-products/sci-](https://www.optalert.com/explore-products/scientifically-validated-glasses-mining/)
571 [entifically-validated-glasses-mining/](https://www.optalert.com/explore-products/scientifically-validated-glasses-mining/). Accessed 27 Aug 2020
- 572 12. Zhang W, Cheng B, Lin Y (2012) Driver drowsiness recognition based on computer vision technology.
573 *Tsinghua Sci Technol* 17(3):354–362
- 574 13. Khessiba S, Blaiech AG, Khalifa KB, Abdallah AB, Bedoui MH (2020) Innovative deep learning models
575 for EEG-based vigilance detection. *Neural Comput Appl* 33:6921–6937
- 576 14. Blaiech AG, Ben Khalifa K, Boubaker M, Bedoui MH (2018) LVQ neural network optimized implementa-
577 tion on FPGA devices with multiple-wordlength operations for real-time systems. *Neural Comput Appl*
578 29:509–528
- 579 15. Boubaker M, Akil M, Ben-Khalifa K, Grandpierre T, Bedoui MH (2010) Implementation of an LVQ
580 neural network with a variable size: algorithmic specification, architectural exploration and optimized
581 implementation on FPGA devices. *Neural Comput Appl* 19(2):283–297
- 582 16. Gromer M, Salb D, Walzer T, Madrid NM, Seepold R (2019) ECG sensor for detection of driver's
583 drowsiness. *Procedia Comput Sci* 159:1938–1946
- 584 17. Zheng WL, Gao K, Li G, Liu W, Liu C, Liu JQ, Wang G, Lu BL (2019) Vigilance estimation using a
585 wearable EOG device in real driving environment. *IEEE Trans Intell Transp Syst* 21(1):170–184
- 586 18. Yeo MV, Li X, Shen K, Wilder-Smith EP (2009) Can SVM be used for automatic EEG detection of
587 drowsiness during car driving? *Saf Sci* 47(1):115–124
- 588 19. Balandong RP, Ahmad RF, Saad MNM, Malik AS (2018) A review on EEG-based automatic sleepiness
589 detection systems for driver. *IEEE Access* 6:22908–22919
- 590 20. Murugappan M, Alshuaib W, Bourisly AK, Khare SK, Sruthi S, Bajaj V (2020) Tunable Q wavelet
591 transform based emotion classification in Parkinson's disease using Electroencephalography. *PLoS ONE*
592 15(11):e0242014
- 593 21. Krishnan PT, Raj ANJ, Balasubramanian P, Chen Y (2020) Schizophrenia detection using Multivariate
594 Empirical Mode Decomposition and entropy measures from multichannel EEG signal. *Biocybern*
595 *Biomed Eng* 40(3):1124–1139
- 596 22. Bajaj V, Taran S, Khare SK, Sengur A (2020) Feature extraction method for classification of alertness
597 and drowsiness states EEG signals. *Appl Acoust* 163:107224
- 598 23. Pfurtscheller G, Flotzinger D, Mohl W, Peltoranta M (1992) Prediction of the side of hand movements
599 from single-trial multi-channel EEG data using neural networks. *Electroencephalogr Clin Neurophysiol*
600 82(4):313–315
- 601 24. Jung TP, Makeig S, Stensmo M, Sejnowski TJ (1997) Estimating alertness from the EEG power spectrum.
602 *IEEE Trans Biomed Eng* 44(1):60–69
- 603 25. Roberts S, Rezek I, Everson R, Stone H, Wilson S, Alford C (2000) Automated assessment of vigilance
604 using committees of radial basis function analysers. *IEE Proc Sci Meas Technol* 147(6):333–338
- 605 26. Vuckovic A, Radivojevic V, Chen AC, Popovic D (2002) Automatic recognition of alertness and drowsi-
606 ness from EEG by an artificial neural network. *Med Eng Phys* 24(5):349–360
- 607 27. Purnamasari PD, Yustiana P, Ratna AAP, Sudiana D (2019) Mobile EEG based drowsiness detection using
608 K-nearest neighbor. In: 2019 IEEE 10th international conference on awareness science and technology
609 (iCAST). IEEE, pp 1–5
- 610 28. He J, Liu D, Wan Z, Hu C (2014) A noninvasive real-time driving fatigue detection technology based on
611 left prefrontal Attention and Meditation EEG. In: 2014 International conference on multisensor fusion
612 and information integration for intelligent systems (MFI). IEEE, pp 1–6
- 613 29. Almogbel MA, Dang AH, Kameyama W (2018) EEG-signals based cognitive workload detection of
614 vehicle driver using deep learning. In: 2018 20th international conference on advanced communication
615 technology (ICACT). IEEE, pp 256–259
- 616 30. Yu S, Li P, Lin H, Rohani E, Choi G, Shao B, Wang Q (2013) Support vector machine based detection of
617 drowsiness using minimum EEG features. In: 2013 international conference on social computing. IEEE,
618 pp 827–835
- 619 31. Bashivan P, Rish I, Heisig S (2016) Mental state recognition via wearable eeg. [arXiv:1602.00985](https://arxiv.org/abs/1602.00985)
- 620 32. Karuppusamy NS, Kang BY (2017) Driver fatigue prediction using eeg for autonomous vehicle. *Adv Sci*
621 *Lett* 23(10):9561–9564
- 622 33. Rohit F, Kulathumani V, Kavi R, Elwarfalli I, Kecojovic V, Nimbarte A (2017) Real-time drowsiness
623 detection using wearable, lightweight brain sensing headbands. *IET Intell Transp Syst* 11(5):255–263
- 624 34. Bakshi V (2018) Towards practical driver cognitive workload monitoring via electroencephalography
625 (Doctoral dissertation)

- 626 35. Foong R, Ang KK, Zhang Z, Quek C (2019) An iterative cross-subject negative-unlabeled learning
627 algorithm for quantifying passive fatigue. *J Neural Eng* 16(5):056013
- 628 36. Nissimagoudar PC, Nandi AV (2020) Precision enhancement of driver assistant system using eeg based
629 driver consciousness analysis & classification. In: Pant M, Sharma TK, Basterrech S, Banerjee C (eds)
630 Computational network application tools for performance management. Springer, Singapore, pp 247–257
- 631 37. Cortes C, Vapnik V (1995) Support-vector networks. *Mach Learn* 20(3):273–297
- 632 38. Alturki FA, AlSharabi K, Abdurraqeab AM, Aljalal M (2020) EEG signal analysis for diagnosing neu-
633 rological disorders using discrete wavelet transform and intelligent techniques. *Sensors* 20(9):2505
- 634 39. Hu B, Li X, Sun S, Ratcliffe M (2016) Attention recognition in EEG-based affective learning research
635 using CFS+ KNN algorithm. *IEEE/ACM Trans Comput Biol Bioinf* 15(1):38–45
- 636 40. Cao LJ, Chua KS, Chong WK, Lee HP, Gu QM (2003) A comparison of PCA, KPCA and ICA for
637 dimensionality reduction in support vector machine. *Neurocomputing* 55(1–2):321–336
- 638 41. Zheng WL, Zhang YQ, Zhu JY, Lu BL (2015) Transfer components between subjects for EEG-based
639 emotion recognition. In: 2015 international conference on affective computing and intelligent interaction
640 (ACII). IEEE, pp 917–922
- 641 42. Zhao C, Zheng C, Zhao M, Tu Y, Liu J (2011) Multivariate autoregressive models and kernel learning
642 algorithms for classifying driving mental fatigue based on electroencephalographic. *Expert Syst Appl*
643 38(3):1859–1865
- 644 43. Goldberger AL, Amaral LA, Glass L, Hausdorff JM, Ivanov PC, Mark RG, Mietus JE, Moody GB,
645 Peng CK, Stanley HE (2000) PhysioBank, PhysioToolkit, and PhysioNet: components of a new research
646 resource for complex physiologic signals. *Circulation* 101(23):e215–e220
- 647 44. Sulaiman N, Taib MN, Aris SAM, Hamid NHA, Lias S, Murat ZH (2010) Stress features identifica-
648 tion from EEG signals using EEG Asymmetry & Spectral Centroids techniques. In: 2010 IEEE EMBS
649 conference on biomedical engineering and sciences (IECBES). IEEE, pp 417–421
- 650 45. Gurudath N, Riley HB (2014) Drowsy driving detection by EEG analysis using wavelet transform and
651 K-means clustering. *Procedia Comput Sci* 34:400–409
- 652 46. Strijkstra AM, Beersma DG, Drayer B, Halbesma N, Daan S (2003) Subjective sleepiness correlates
653 negatively with global alpha (8–12 Hz) and positively with central frontal theta (4–8 Hz) frequencies in
654 the human resting awake electroencephalogram. *Neurosci Lett* 340(1):17–20
- 655 47. Khare SK, Bajaj V (2020) Optimized tunable Q wavelet transform based drowsiness detection from
656 electroencephalogram signals. *IRBM*
- 657 48. Neffati S, Ben Abdellafou K, Taouali O, Bouzrara K (2020) Enhanced SVM–KPCA method for brain
658 MR image classification. *Comput J* 63(3):383–394
- 659 49. Scholkopf B, Smola AJ (2018) Learning with kernels: support vector machines, regularization, optimiza-
660 tion, and beyond. Adaptive computation and machine learning series. The MIT Press, Cambridge
- 661 50. Abidi A, Nouria I, Aasali I, Saafi MA, Bedoui MH (2021) Hybrid multi-channel EEG filtering method
662 for ocular and muscular artifact removal based on the 3D spline interpolation technique. *Comput J*
- 663 51. Rahma ON, Rahmatillah A (2019) Drowsiness analysis using common spatial pattern and extreme learning
664 machine based on electroencephalogram signal. *J Med Signals Sens* 9(2):130
- 665 52. Belakhdar I, Kaaniche W, Djemal R, Ouni B (2018) Single-channel-based automatic drowsiness detection
666 architecture with a reduced number of EEG features. *Microprocess Microsyst* 58:13–23
- 667 53. Tripathy RK, Acharya UR (2018) Use of features from RR-time series and EEG signals for automated
668 classification of sleep stages in deep neural network framework. *Bio cybern Biomed Eng* 38(4):890–902
- 669 54. Correa AG, Leber EL (2010) An automatic detector of drowsiness based on spectral analysis and wavelet
670 decomposition of EEG records. In: 2010 annual international conference of the IEEE engineering in
671 medicine and biology. IEEE, pp 1405–1408
- 672 55. Albalawi H, Li X (2018) Single-channel real-time drowsiness detection based on electroencephalography.
673 In: 2018 40th annual international conference of the IEEE engineering in medicine and biology society
674 (EMBC). IEEE, pp 98–101
- 675 56. Xiong YJ, Zhang R, Zhang C, Yu XL (2013) A novel estimation method of fatigue using EEG based
676 on KPCA-SVM and complexity parameters. In: Applied mechanics and materials, vol 373. Trans Tech
677 Publications Ltd, Bäch, pp 965–969
- 678 57. Anitha C (2019) Detection and analysis of drowsiness in human beings using multimodal signals. In:
679 Patnaik S, Yang X-S, Tavana M, Popentiu-Vlădicescu F, Qiao F (eds) Digital business. Springer, Cham,
680 pp 157–174
- 681 58. Ogino M, Mitsukura Y (2018) Portable drowsiness detection through use of a prefrontal single-channel
682 electroencephalogram. *Sensors* 18(12):4477
- 683 59. Gwak J, Shino M, Hirao A (2018) Early detection of driver drowsiness utilizing machine learning based
684 on physiological signals, behavioral measures, and driving performance. In: 2018 21st international
685 conference on intelligent transportation systems (ITSC). IEEE, pp 1794–1800

- 686 60. Breitenbach J, Baumgartl H, Buettner R (2020) Detection of excessive daytime sleepiness in resting-
687 state EEG recordings: a novel machine learning approach using specific EEG sub-bands and channels.
688 AMCIS'20 Proceedings
- 689 61. Lan K-C, Chang D-W, Kuo C-E, Wei M-Z, Li Y-H, Shaw F-Z, Liang S-F (2015) Using off-the-shelf lossy
690 compression for wireless home sleep staging. *J Neurosci Methods* 246:142–152
- 691 62. Jeong JH, Yu BW, Lee DH, Lee SW (2019) Classification of drowsiness levels based on a deep spatio-
692 temporal convolutional bidirectional LSTM network using electroencephalography signals. *Brain Sci*
693 9(12):348
- 694 63. Wang Q, Li Y, Liu X (2018) Analysis of feature fatigue EEG signals based on wavelet entropy. *Int J*
695 *Pattern Recogn Artif Intell* 32:1854023
- 696 64. Hjorth B (1970) EEG analysis based on time domain properties. *Electroencephalogr Clin Neurophysiol*
597 29(3):306–310
- 698 65. Vourkas M, Micheloyannis S, Papadourakis G (2000) Use of ann and hjorth parameters in mental-task dis-
699 crimination. In: 2000 first international conference advances in medical signal and information processing
700 (IEE conference publication No. 476). IET, pp 327–332
- 701 66. Krishnan P, Yaacob S (2019) Drowsiness detection using band power and log energy entropy features
702 based on EEG signals. *Int J Innov Technol Explor Eng* 8:10
- 703 67. Vimala V, Ramar K, Ettappan M (2019) An intelligent sleep apnea classification system based on EEG
704 signals. *J Med Syst* 43(2):36

705 **Publisher's Note** Springer Nature remains neutral with regard to jurisdictional claims in published maps and
706 institutional affiliations.